Performance-based assessment of a steel lattice power-transmission tower: A case study in Germany

Dimitrios V. Bilionis[1]

RISA Sicherheitsanalysen GmbH, Xantener Straße 11, Berlin-Wilmersdorf 10707, Germany

Konstantinos Vlachakis

Institute of Steel Structures, National Technical University of Athens, Athens 15780, Greece

Marios-Zois Bezas

Steel and Composite Construction, UEE Research Unit, University of Liège, Liège 4000, Belgium

Mike Tibolt

ArcelorMittal Steligence®, Esch-sur-Alzette 4009, Luxembourg

Dimitrios Vamvatsikos, Ioannis Vayas

Institute of Steel Structures, National Technical University of Athens, Athens 15780, Greece

ABSTRACT

Power transmission towers are tall steel lattice structures used for supporting the conductors of a power transmission line, constituting essential parts of an entire power network. Past experience has shown that even a failure of a single tower can cause cascading effects to its adjacent towers leading to a total collapse of a whole line. Transmission towers are susceptible to severe weather conditions including low temperatures, snow and high winds. Specifically, high winds in combination with ice accumulation increase the lateral and vertical loads to levels causing damages ranging from local failures to global collapse. This effect is even more intense in case of aged towers with members weakened by corrosion effects. Herein, the focus is on a single suspension transmission tower widely used in Central Europe and designed according to the EN 50341-1:2012 and EN 50341-2-4:2016 assuming installation in Germany. The structure's fragility in both initial and corroded state against wind and icing loads was estimated via nonlinear dynamic analyses. The climatic hazard was estimated by deriving the joint probability of wind speed and ice thickness based on meteorological data obtained for Central-East Germany. Finally, the assessment of the structure's risk for each of the two states considered was made by combining the tower's fragility results with the climatic hazard. Assessing the risk of a single tower is a precursor of estimating the reliability of an entire power transmission network, offering a useful decision-support tool on the need to maintain or upgrade a power line network.

Keywords: Power transmission tower, Wind, Ice, Steel lattice tower, Corrosion

INTRODUCTION

Power transmission lines are essential parts of a region's infrastructure. A transmission line is actually a system of various structures whose undisrupted operation ensures the continuous supply of electricity to consumers. Transmission towers are tall steel structures used for supporting the conductors of a power line. Those towers constitute a very crucial component of a power line. A failure or collapse of a tower may result in major power outages with commensurate economic and social consequences.

Transmission towers are susceptible to extreme meteorological conditions. Experience has shown that events of adverse weather can lead to tower collapses with long electricity outages (Klinger et al., 2011). For this

---

[1] d.bilionis@risa.de

reason, the analysis of these structures has gathered much attention in the literature, especially in today's era of climatic change, which makes adverse weather events throughout the world more often than in the past. A number of studies investigating the response of transmission towers and lines especially under strong winds have been published (Fu et al., 2019; Fu et al., 2016; Zhang et al. 2015; Darestani et al., 2019; Rezaei et al. 2017). However, despite those efforts there is still a need for expansion of relevant research especially towards the development of a performance-based framework that could provide power network operators with a useful tool in decision making regarding their network operation, maintenance and expansion.

Considering the above, a case study of performance-based assessment of a power transmission tower is presented. The tower is designed according to the EN 50341-1:2012 and EN 50341-2-4:2016 and its location is assumed in the eastern part of Germany. Herein, two states are considered: the initial state (i.e., brand new) and its expected state after 60 years of service considering the effects of corrosion. First, the fragility of the structure due to wind and icing conditions is assessed for both states. Then the climatic hazard of the site of installation is estimated by elaborating meteorological data from the nearest meteorological station. Finally, the probability of failure (i.e. risk) of the tower in each state is estimated by combining the results of fragility analyses with the climatic hazard.

TOWER MODEL

Geometry

A standard Danube tower widely used in Central Europe is considered in the present case study. It has been designed according to EN 50341-1:2012 and EN 50341-2-4:2016 for the case of Germany. The tower has a standard height of 50m and two cross-arms with different lengths. The lower cross-arm's length is 31m while the upper's is 22m. The main body of the tower has square cross-section (6.84m by 6.84m at the base) whose dimensions reduce with height. Figure 1 shows the tower configuration separated in a number of segments along its height. The tower members are made by hot-dip galvanized equal-leg angle profiles of various sizes.

The tower is assumed to be a suspension (support) tower carrying two 380 kV circuits each of them consisting of three phases. Each phase is made of a bundle of four conductors supported by a suspension insulator hanging vertically. Furthermore, a single earth-wire is installed on the top of the tower for lighting protection. The type 264-AL1/34-ST1A was selected for conductors, while 94-AL1/15-ST1A is employed for the earth-wire. Finally, the Quadril*Sil insulator S025185S201 made of silicone rubber having a length of 5m and a weight of 87N (i.e. 9 kg) was selected. A detailed description of the tower's geometry and additional specifications are provided in Bezas et al. (2019) and Tibolt et al. (2021).

Material

The structural steel grade is S355J2 for all the members of the tower. At this point it should be noted that since the goal is not the design but a performance assessment for a power transmission tower, the expected values of steel strength were employed in the model, instead of the nominal ones. Specifically, for steel grade S355J2, the (mean) yield strength f_y is equal to 454.90 MPa and the (mean) tensile strength f_u is equal to 546.84 MPa (Braconi et al, 2013). The material stress-strain curve that was assumed in the analysis is presented in Figure 2. The Young Modulus of steel is taken as E=210 GPa. Fiber sections were employed together with beam-column and truss elements to model the tower. To assign stress-strain relationships to each steel fiber, the general form of Figure 2 was employed as stress-strain curve in compression and tension, using the buckling reduction factor χ, as calculated for each structural member according to EN 1993-3-1, to account for compression buckling.
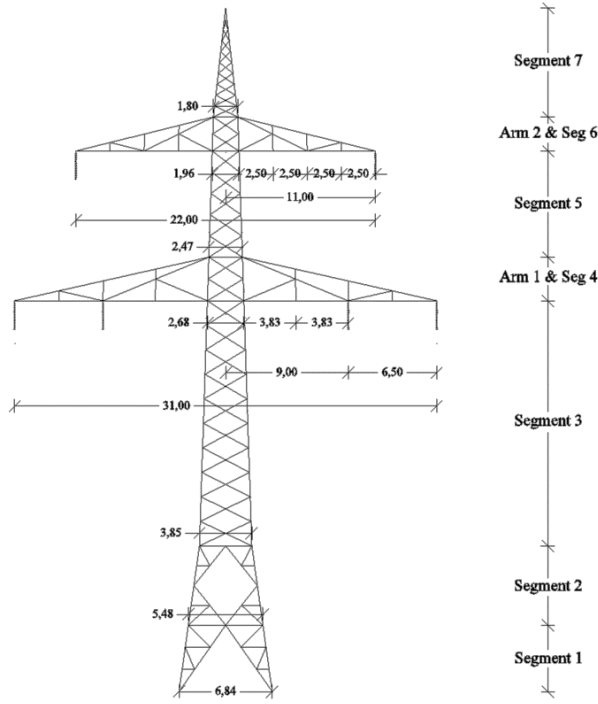
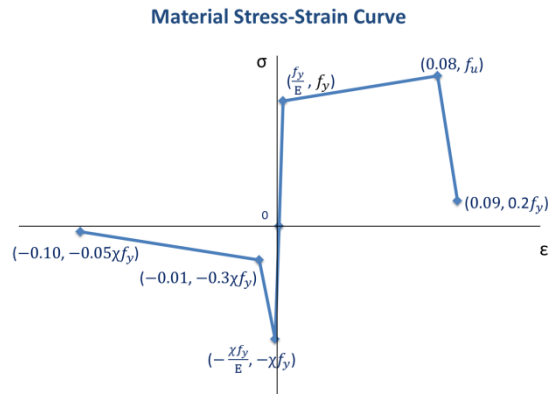**Figure 1.** *Danube tower configuration (Source: Bezas et al, 2019)*

Figure 2. *General form of a member stress-strain curve*

Loads

Dead Loads

The total weight of all tower members was calculated after multiplying the length of each member by the corresponding unit weight of the member's angle profile resulting in a total of approximately 166.61 kN (i.e. 16.99 tons). For each of the six insulators considered in the model the weight was estimated to be 87 N, resulting in a total weight of 522 N (i.e. 53.23 kg).

Wind Loads

The wind force acting on the tower is calculated as:

$$F_{tower} = qC_D A_{ref} \tag{1}$$

where q is the dynamic pressure of the wind, C_D is the drag coefficient and A_{ref} is the area of the members projected normal to the level of the wind. The dynamic pressure of the wind q depends on the air density ρ and the wind speed u and is estimated using the following expression:

$$q = \frac{1}{2}\rho u^2 \tag{2}$$

Herein, ρ is assumed to be equal to 1.25 kg/m^3.

The drag coefficient C_D for lattice steel structures depends on the solidity ratio φ. According to EN1991-1-4, the solidity ratio φ is the fraction of the sum of the projected area A of the members of the structure's face normal to that face divided by the total area A_c enclosed by the face's boundaries projected normal to that face. Thus:

$$\varphi = \frac{A}{A_c} \tag{3}$$

Eq. (3) was applied to each of the segments of the tower as presented in a previous section. In specific, each of the segments was divided into sub-segments of approximately 1.5m height. Then, the solidity ratio φ of each sub-segment was calculated and the corresponding drag coefficient was estimated based on EN1991-1-4. The resulting wind force was estimated using Eq. (1) and (2) and considering the corresponding wind speed for each sub-segment based on its height. Finally, the wind force was assigned to the corner nodes of each sub-segment.

Ice Loads
Apart from wind, another environmental hazard that should be taken into account is ice. In the case of a steel lattice transmission tower, ice accumulates on the surface of the exposed structural members. It is important to note that the EN 50341-1:2012 does not consider any ice accumulation on the tower structure but only on the conductors. However, ice accretion affects the loads of the structure, by increasing both the weight (i.e. dead load) and the projected area of the members. Following the previous section, where the estimation of the wind loads was discussed, it can be inferred that an increase in the projected area of the members affects the solidity ratio of the tower and the corresponding drag coefficients resulting in a larger wind force for the same wind speed value.

Herein, it was assumed that an ice layer of uniform thickness can be formed on the surface of the exposed parts of the members and the conductors. In terms of the value of the ice thickness, four scenarios of different values were considered, namely 1mm, 5mm, 10mm, and 15mm. For each of those icing scenarios, the corresponding areas of the ice surface and the associated values of the affected parameters (e.g. weight, solidity ratio etc.) were estimated. Finally, it should be noted that the unit weight of ice was considered equal to 7.355 kN/m^3 as adopted by EN 50341-1:2012.

Conductor and Insulator Loads
When a conductor is suspended between two points (e.g. two insulators of adjacent towers) it forms a catenary curve (Kiessling et al, 2003; Cuchapin, 2018). The mathematical expression of this curve is given by the following equation:

$$y = C\left(\cosh\frac{x}{C} - 1\right) \tag{4}$$

where:

$$C = \frac{H}{W} \tag{5}$$

H is the horizontal tension force and W the weight of the conductor.

The total force acting at the end of the conductor, T_{supp}, is calculated by combining the horizontal and vertical reaction, T_x, T_y (Figure 3a) as follows:

$$T_x = H \tag{6}$$
$$T_y = \frac{wL}{2}$$
$$T_{supp} = \sqrt{T_x^2 + T_y^2}$$

Both wind and ice have a significant effect on the conductor's sag and tension. Assuming that a layer of ice thickness t (Figure 3b) has been formed around the conductor, then the additional weight W_{ice} due to ice is calculated as:

$$W_{ice} = \rho_{ice} V_{ice} = \rho_{ice} \pi t(D + t) \tag{7}$$

where ρ_{ice} is the ice density and D the diameter of the conductor.

If at the same time a wind speed u over the above conductor is applied, then the additional force W_{wind} per unit length due to wind is:

$$W_{wind} = q(D + 2t) \tag{8}$$

where: q is the dynamic pressure of the wind estimated by Eq. (2).

Thus, the total force per unit length due to conductor's own weight, wind and ice is equal to:

$$W_{total} = \sqrt{(W + W_{ice})^2 + W_{wind}{}^2} \tag{9}$$

When the conductor is installed (i.e. strung) it obtains an initial horizontal tension H_1 which is mainly affected by the temperature during installation. The final tension H_2 in the conductor including the effect of ice and wind is calculated by solving the following Equation, assuming a parabolic sag-line of the conductor:

$$H_2{}^3 + H_2{}^2 \left(\frac{(W_1 S)^2 AE}{24 H_1{}^2} - H_2 + (t_2 - t_1)aAE \right) - \frac{(W_2 S)^2 AE}{24} = 0 \tag{10}$$

W_1 is the unit weight of the conductor at initial temperature, W_2 is the unit weight of the conductor at final temperature (i.e. to be taken as the total unit force W_{total} to also account for wind and ice), t_1 and t_2 are the initial and final temperature (ºC) respectively, S is the span length, a is the coefficient of linear thermal expansion, E is the conductor's modulus of elasticity, and A is the conductor's cross-sectional area.

Herein, the span length was assumed equal to 350m, the initial temperature 10ºC and the final temperature 10ºC for the no ice conditions and -1ºC for the icing conditions. The tension and the sag of the conductors and the earth-wire were estimated for various values of wind speeds and ice thicknesses described in a following section. Finally, based on the above equations, the loads due to conductors and earth-wire were estimated and applied in the model of the tower. It should be noted that the aforementioned equations are valid for one bundle, thus for the case at hand (four-bundled conductors) the results were multiplied by four.

The wind force at an insulator F_{ins} is simply estimated by applying the following equation:
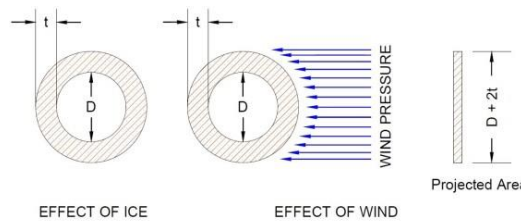
$$F_{ins} = q C_D A_{ref} = q C_D (D_{ins} + t) \tag{11}$$

Where q is the dynamic pressure of the wind, D_{ins} is the diameter of the insulator, t is the ice thickness (if applicable) and C_D the drag coefficient assumed here equal to 1.20.

a)
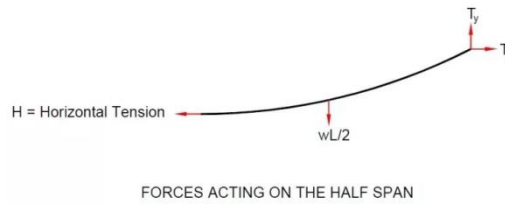
b)

Figure 3. a) Forces acting at half span of a conductor, b) Effects of ice and wind (Source: Cuchapin, 2018)

Effect of Corrosion
Corrosion is an important aging factor which contributes significantly to the degradation of the strength of steel members. Corrosion mainly reduces the cross-section parameters, such as size, area and moment of

inertia. Thus, the overall strength of the structures weakens. Corrosion rate, i.e. the annual loss of cross-section reduction depends on various parameters such as the type of material (i.e. carbon steel, weathering steel, zinc, etc.) and the atmospheric environment of the structure. International standards (EN 12500:2000; EN ISO 9223; EN ISO 9224; EN ISO 9225; EN ISO 9226) provide the classification of atmospheric environment and the corresponding typical values for corrosion rates.

For the case at hand, the environment of installation was assumed to be of category C3 (medium corrosivity) according to EN ISO 9226. The corresponding corrosion rates were assumed to be $r_{av} = 2$ μm/yr for the zinc layer, and $r_{av} = 12$ μm/yr and $r_{lin} = 6$ μm/yr for the carbon steel based on EN ISO 9224. The thickness of the zinc layer was assumed to be equal of 40μm, thus it is expected to be exhausted during the first 20 years of service. The resulting carbon steel loss that will follow is presented in Figure 4. Finally, assuming a service life of 60 years, the estimated loss of thickness for carbon steel at the end of the service life is 0.3mm.
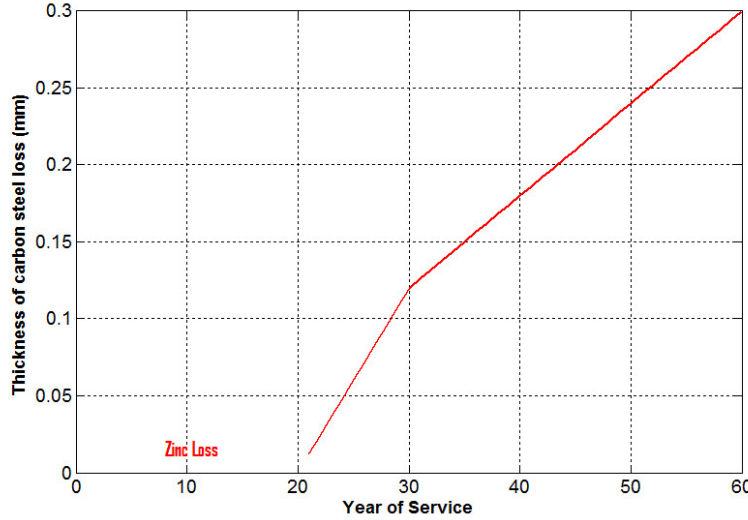
Figure 4. *Loss of thickness during service life of the suspension transmission tower*

TOWER MODEL

OpenSees Model
For the analysis, the tower was modelled in OpenSees, an open-source structural analysis platform (Mazzoni et al, 2006). The final 3D model was composed of 982 members, simulated as truss or beam elements with fiber sections having appropriately calibrated stress-strain relationships. Since the tower is considered to be a suspension tower, it is assumed that it will not take any tension loads due to conductors along the line direction. Thus, only the transverse and vertical loads due to conductors were simulated by applying the corresponding forces on the location of the insulators. On the other hand, the earth-wire is directly connected on the tower, transferring not only vertical but also lateral forces; thus its effect was simulated via a horizontal spring as proposed by Fu et al. (2016). The stiffness of the spring is estimated according to Veletsos & Darbre (1983) as follows:

$$k_c = \frac{1}{1+p} \frac{AE}{L_e} \cos^2 \theta + \frac{T_o}{L} \sin^2 \theta \tag{12}$$

$$p = \frac{1}{12} \frac{AE}{T_o} \frac{L}{L_e} \left(\frac{q_y L}{T_o}\right)^2 \tag{13}$$

A and E are the cross-sectional area and the elastic modulus of the earth-wire, respectively, θ is the inclination angle of the earth-wire, T_o is the earth-wire's tension, L_e is the effective length equals to $L \times \left[1 + 8 \times \left(\frac{sag}{L}\right)^2\right]$, where L is the span length and q_y is the normal load per unit of earth-wire's length.

Based on the above, the spring stiffness depends not only on the wire's characteristics but also on the wind speed acting on it. Since the estimation of the spring stiffness for all the wind speed values considered in the analyses would require a large computational effort slowing down the analysis procedure, the spring stiffness was calculated using the basic wind speed ($V_b = 25$ m/s) of the tower's location as provided by the German

National Annex of EN 50341-1:2012. In total, five different versions were analyzed, one for no icing conditions and one for each of the four different scenarios of ice thickness as presented earlier.

Modal Analysis

The natural frequencies of the structure were determined by a modal analysis. The first two modes are longitudinal (directions X and Y) and the third mode is torsional. Modal analyses were also performed for each of the icing scenarios. Table 1 presents the periods of the first three modes for each of the five scenarios considered herein. The results show, as expected, that as the thickness of the ice layer increases, the corresponding periods increase. Certainly, this should be attributed to the increase of the tower mass. Furthermore, since corrosion reduces the size of the angle cross-sections, it also reduces the stiffness of the tower. Thus, as shown in Table 1, the corroded tower has higher periods than the initial one.

Table 1. Natural periods of the first three modes for all icing scenarios for initial and corroded towers

Ice Thickness (mm)	Initial Tower			Corroded Tower		
	T_1 (s)	T_2 (s)	T_3 (s)	T_1 (s)	T_2 (s)	T_3 (s)
0	0.511	0.504	0.434	0.526	0.518	0.466
1	0.520	0.513	0.440	0.534	0.526	0.471
5	0.559	0.548	0.464	0.574	0.561	0.498
10	0.605	0.597	0.495	0.622	0.613	0.531
15	0.656	0.646	0.526	0.673	0.663	0.564

Wind Speed Simulation

Wind Speed Profile
Wind speed increases with height following a specific pattern known as the wind speed profile. Herein, a power law wind speed profile was considered, according to which the value of wind speed at a height z is given by:

$$\frac{u}{u_{ref}} = \left(\frac{z}{z_{ref}}\right)^{a} \tag{14}$$

where: u is the wind speed at height z, u_{ref} is the wind speed at a reference height z_{ref} and a is the power law exponent. Herein, a power law exponent $a = 0.20$ was used, as proposed by IEC 61400-1 for onshore structures. Eq. (14) gives the values of the wind speed of the reference points for each sub-segment along the height of the tower. Based on these values, the corresponding wind force along the height of the tower is estimated by applying Eq. (1).

Wind Field Simulation
The simulation of the wind field around the tower was performed in the TurbSim software (Jonkman & Klinger, 2012). TurbSim has been developed by National Renewable Energy Laboratory (NREL) of the USA and is mainly used in wind turbine applications. The software simulates a 2D wind field over a custom grid whose dimensions and resolution are specified by the user, generating timeseries of wind speed in the X, Y, Z axes over a user-defined period (e.g. 10 min, 1 hour etc.) and for a specific mean wind speed (reference wind speed). Thus, in the case of a transmission tower, the grid provides the capability of simulating the wind speed not only along a single transmission tower's profile but also along the conductors' length (i.e. span). For each of the two horizontal axes, the corresponding X, Y wind force timeseries (ignoring the vertical wind component which was of negligible magnitude) were estimated by applying Eq. (1) for the reference points of the sub-sections along the height of the tower. Furthermore, values of wind speed were estimated for a number of specific points (every 50m) along each span of the considered transmission line in order to estimate the wind forces acting on the conductors and earth-wire following the methodology discussed in a previous section. It is noteworthy that the timeseries created by Turbsim fully model the frequency content of the wind excitation, explicitly incorporating any changes due to wind speed characteristics.
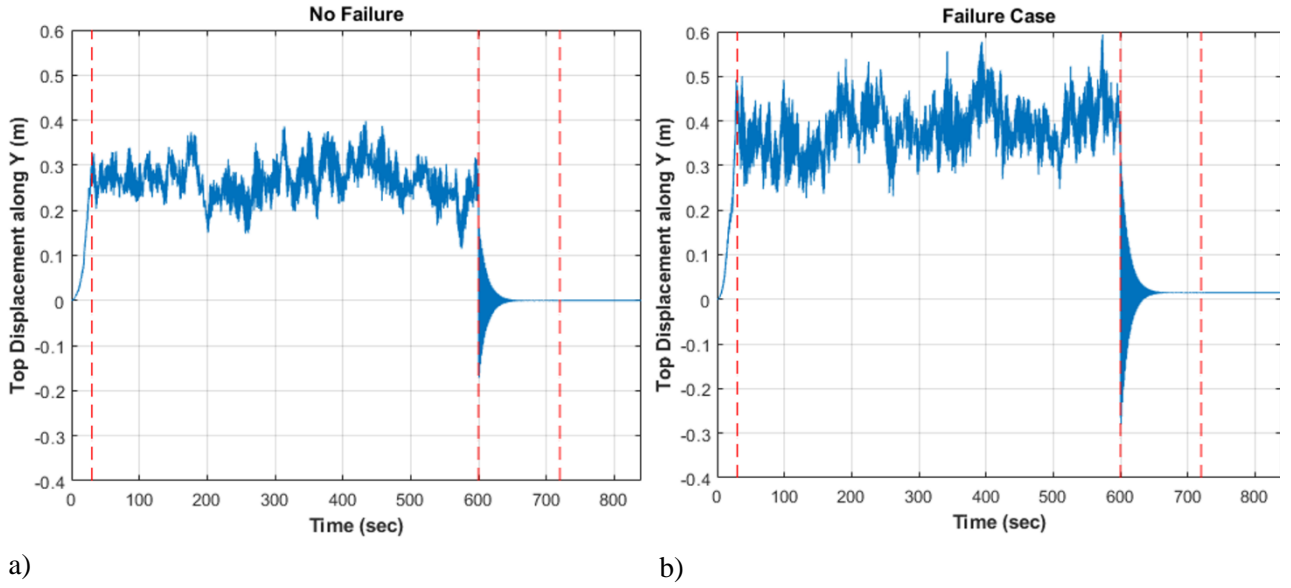
Dynamic Analysis

The main input for the nonlinear dynamic analysis was the timeseries of the wind speed created in TurbSim as discussed above. Thus, the wind speed timeseries were estimated at points every 1m along the height of the tower and every 50m along the length of the conductors and the earth-wire. Figure 5(a) presents a typical form of the wind speed timeseries. The length of each timeseries was 10 minutes. The estimation of the wind forces on the body of the tower was made by processing the results of the wind speed timeseries and performing the necessary calculations by applying Eq. (1) along the two horizontal directions (longitudinal and transverse to the line) of the tower. The wind forces at the conductors and the earth-wire were estimated following the methodology presented in a previous subsection. Those values constituted the inputs of the dynamic parameters for the OpenSees software where the dynamic analysis was performed. A typical form of wind force timeseries is presented in Figure 5(b). It is noteworthy, that the wind force was ramped up gradually during the first 30sec of the analysis to avoid any transient artefacts arising from the sudden application of a high wind load.

a)   b)
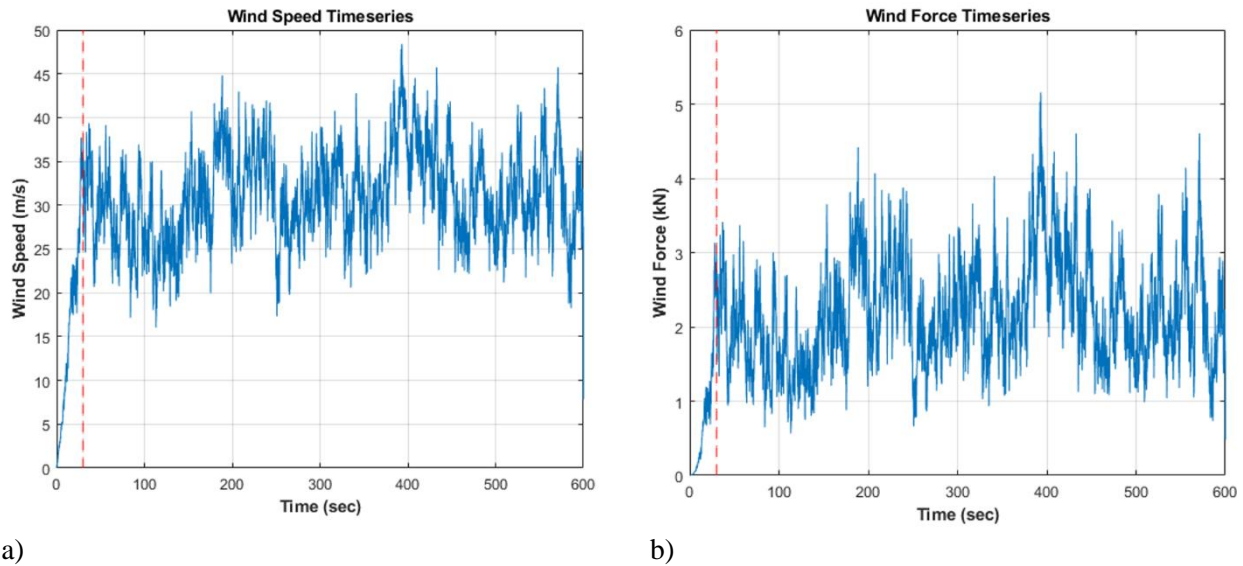
Figure 5. *a) Typical wind speed timeseries and b) Typical wind force timeseries*
The added ramp-up appears before the 30sec mark indicated by the red dashed line

Figure 6 presents typical forms of timeseries resulted after each dynamic analysis in OpenSees. It is noteworthy that each dynamic analysis had a length of 840 sec (14 min) and could be divided into four phases. During the first phase (0-30 sec) the wind load was gradually applied (ramp-up) as mentioned above. The second phase (30-600 sec) was the main phase of the dynamic analysis where the full loads (dynamic and static) were applied. In the third phase (600-720 sec), a zero-wind speed was considered and hence the tower was at free oscillation. Finally at the fourth phase (720-840 sec), the weights of conductors and earth-wire have been removed thus the tower carries only its own weight and the weight of the ice layer, if any. The no-conductors phase was included in the analysis in order to highlight any residual displacements on the tower body considering no horizontal or vertical forces (apart from the tower members weight). The distinction in the above phases was selected in order to assess whether a failure occurred. For instance, if one considers a point on the structure (e.g., the top), in a case where no failure is observed the displacement at that point during the fourth phase (720-840 sec) should be zero (*Figure 6*a). On the other hand, if a permanent failure occurs, a residual displacement different from zero should be observed (*Figure 6*b). In general, the tower fails in a brittle and dramatic way due to member buckling. Therefore, only the limit-state of global collapse is considered. The above process provides a simple and quick way to determine failure by observing the displacements of selected points (e.g. joints) along the height of the structure. Furthermore, it reduces the computational effort and the analysis time of recording and post-processing the internal forces or stresses and strains for all members (close to 1,000) of the structure.

Figure 6. *Typical timeseries of top displacement in the transverse direction (along Y) for: a) a non-failure case and b) a failure case*

FRAGILITY ESTIMATION

The results of the dynamic analyses were used for the estimation of fragility of the tower to wind and/or icing conditions. Fragility could be defined as the probability of failure for a given (scalar or vector) intensity measure (IM). The results of such an analysis are reported in the form of fragility curves. The estimation of the fragility functions and corresponding curves is based on the probability of failure for the various values of the IM. A common assumption is that the fragility curve is defined by a lognormal cumulative function (CDF) with the following mathematical expression (Baker, 2015):

$$P(D > C|IM = x) = \Phi\left(\frac{ln\left(\frac{x}{x_{50}}\right)}{\beta}\right) \tag{15}$$

where: $P(C|IM = x)$ is the probability that a value of the IM (e.g. the wind speed) equal to x will cause a failure of the structure (i.e., demand exceeds capacity, $D > C$), $\Phi(\cdot)$ is the standard normal cumulative distribution function (CDF), x_{50} is the median of the fragility function which corresponds to the value of IM with 50% probability of failure and β is the standard deviation of $\ln IM$, sometimes referred to as dispersion of IM.

For the case at hand, the IM has three components, namely: wind speed (u), wind direction (θ) and ice thickness (t). Thus, for each of the towers (initial and corroded), a two-parameter fragility was estimated via a multi-stripe approach (Jalayer & Cornell, 2009). In specific, for each icing scenario, discrete levels of u were selected within the range 17 – 35 m/s at steps of 1 m/s, while three different wind angles of attack, namely: 0° (along the line), 45° and 90° (transverse to the line) were deemed to be sufficient for capturing practically all wind angle effects due to the symmetry of the towers and conductors. At each combination (or "stripe") of u and θ considered and for specific ice thickness, twelve wind-speed timeseries were found to be more than sufficient for the analysis due to the low record-to-record variability. The above process was applied for both towers of study: initial and corroded. Finally, the probability of failure at the given vector IM value of (u, θ, t), or $P(D > C|u, \theta, t)$, can be estimated as the fraction of analyses causing failure over the total of 12 (Bakalis & Vamvastikos, 2018).

Given the probability of failure for the combinations (u, θ, t), the corresponding fragility curve can be derived by fitting a lognormal function (Eq. 15) as follows:

$$P(D > C|u, \theta, t) = \Phi \left(\frac{ln\left(\frac{x}{u_{50}(\theta, t)}\right)}{\beta(\theta, t)} \right) \tag{16}$$

Where: $u_{50}(\theta, t)$ is the median of the fragility function which corresponds to the value of *IM* with 50% probability of failure and $\beta(\theta)$ is the logarithmic standard deviation, referred to as *dispersion* of the *IM* failure capacity. The dispersion estimated from fitting the lognormal distribution to the fragility for each wind direction and ice thickness, termed $\beta_R(\theta, t)$, can be augmented to account for additional sources of uncertainty by taking a first-order assumption (Cornell et al., 2002). Then, additional uncertainty does not change the central value (median) of the capacity distribution, only increasing its dispersion in a square-root-sum-of-squares fashion:

$$\beta(\theta, t) = \sqrt{\beta_R(\theta, t)^2 + \beta_b^2} \tag{17}$$

where: $\beta_R(\theta, t)$ is the dispersion estimated from the (dynamic) analyses ranging from 0.01 to 0.03 and $\beta_u = 0.10$ the dispersion attributed to member tests for steel angle buckling resistance (Paschen et al, 1988).

Figure 7 shows the fragility curves of the five scenarios of ice thickness considered. It is obvious that the position of the fragility curve moves to the left as the ice thickness increases. This means that as ice accumulates on the tower and the conductors, the median wind speed of failure decreases. This finding should be attributed to the impact that ice has on the structure by increasing both the dead loads and the wind force for a given wind speed. Moreover, as expected, the median wind speed of failure for a specific combination of wind angle and ice thickness in the case of the corroded tower is lower than in the initial tower. A finding that is due to the lower strength of the aged tower.
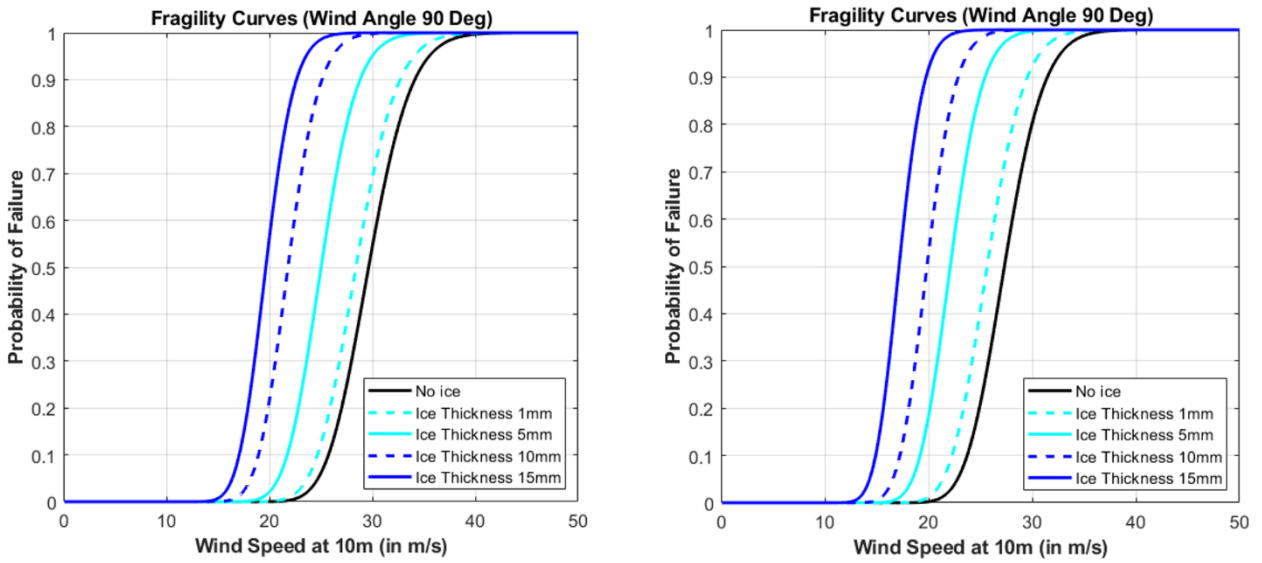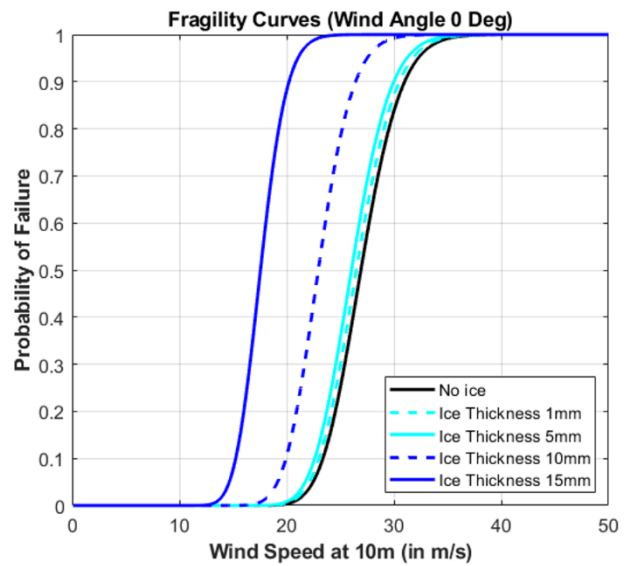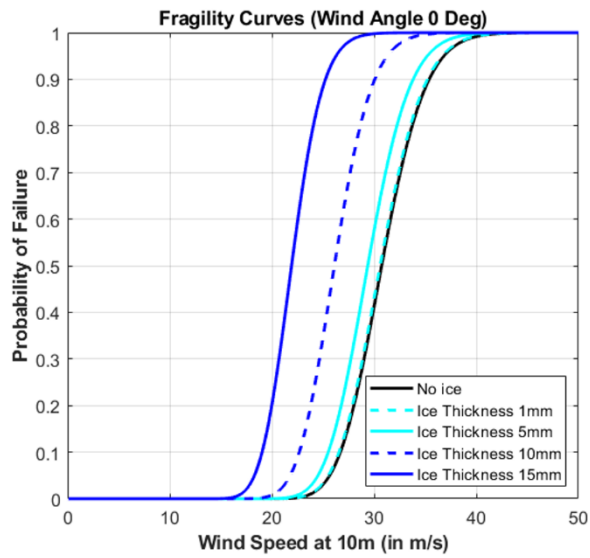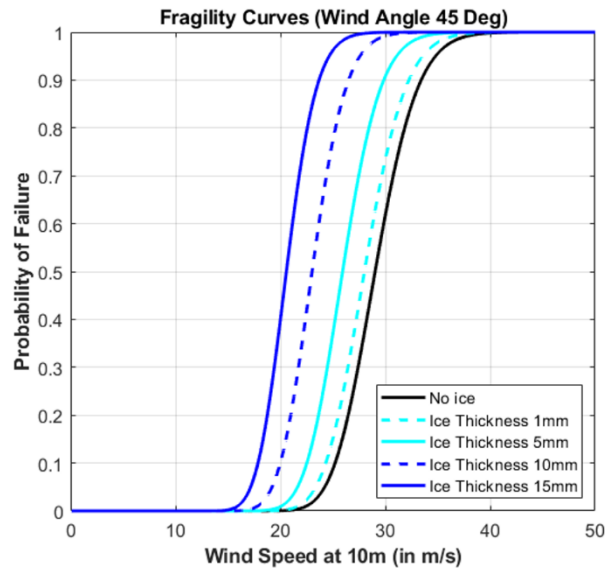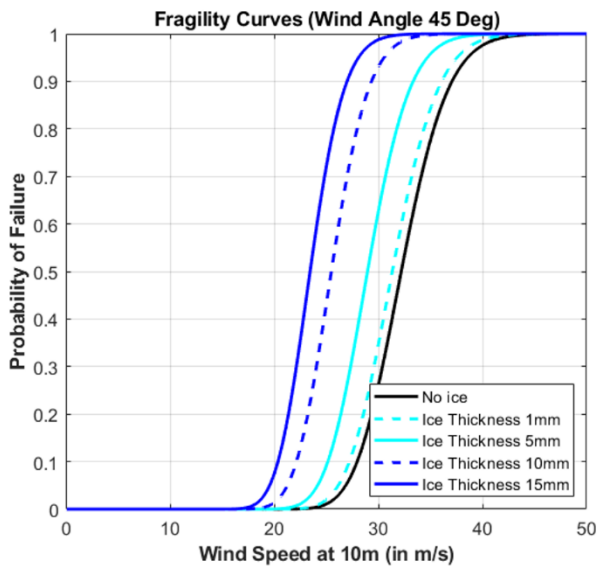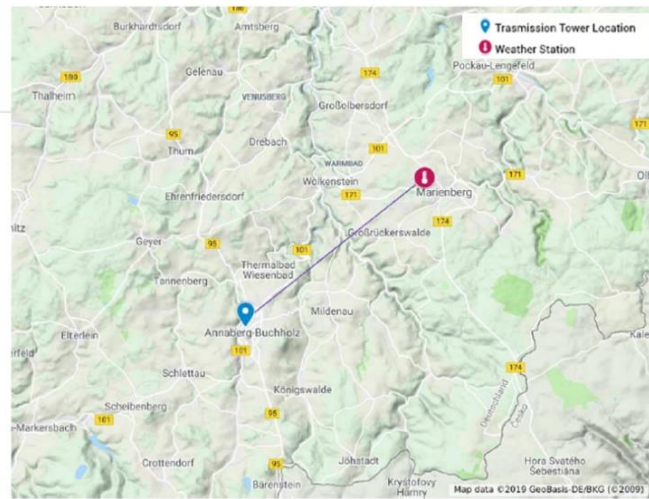
Figure 7. Fragility curves for the initial tower (left) and for the corroded tower (right)

CLIMATIC HAZARD

The climatic hazard addresses the frequency of adverse weather conditions occurring at a specific site. Herein, the site of installation of the transmission tower is Annaberg-Buchholz, Germany, as shown in the map of Figure 8.

Figure 8. *Location of the tower and weather station*

Meteorological Data

For the estimation of the climatic hazard, meteorological data from the closest weather station should be obtained. The closest weather station to the site of installation is the station located in Marienberg at a distance of 13km, as shown in Figure 8. The station is operated by the German Weather Service (Deutscher Wetterdienst – DWD) and provides detailed meteorological information over a long period of time freely available online (https://www.dwd.de).

Detailed timeseries of wind speed (measured at 10m) are available in 10min resolution. Figure 9 shows the wind speed distribution and the wind rose for the site of Marienberg. It can be inferred from Figure 9a that the majority of observations is lower than 5 m/s. In addition, the mean wind speed observed was 2.96 m/s with a standard deviation of 1.95 m/s. Finally, the probability of calm conditions was around 4.34%. In terms of wind direction, the wind rose (Figure 9b) shows that the dominant wind direction is W (wind angle of 270°). Except for W, very high frequency (close to 20%) shows the direction SW (225°). All the rest of directions show frequencies less than 10% each.

In terms of the icing conditions due to the absence of measured data, the method of equivalent ice thickness R_{eq} was used as proposed by Jones (1998). The statistical analysis of the ice results revealed that the probability of ice conditions at the site of interest is 18.89%. Figure 10 shows the distribution of the estimated ice thicknesses. It is noteworthy that the heights of the columns correspond to ice conditions (i.e., zero ice thickness was exported) which correspond to 18.89% of time. So, the values of z-axis were multiplied by 0.1889. It is observed that the vast majority of ice thickness was lower than 10mm, with a mean value of 5.86mm and a standard deviation of 7.35mm.
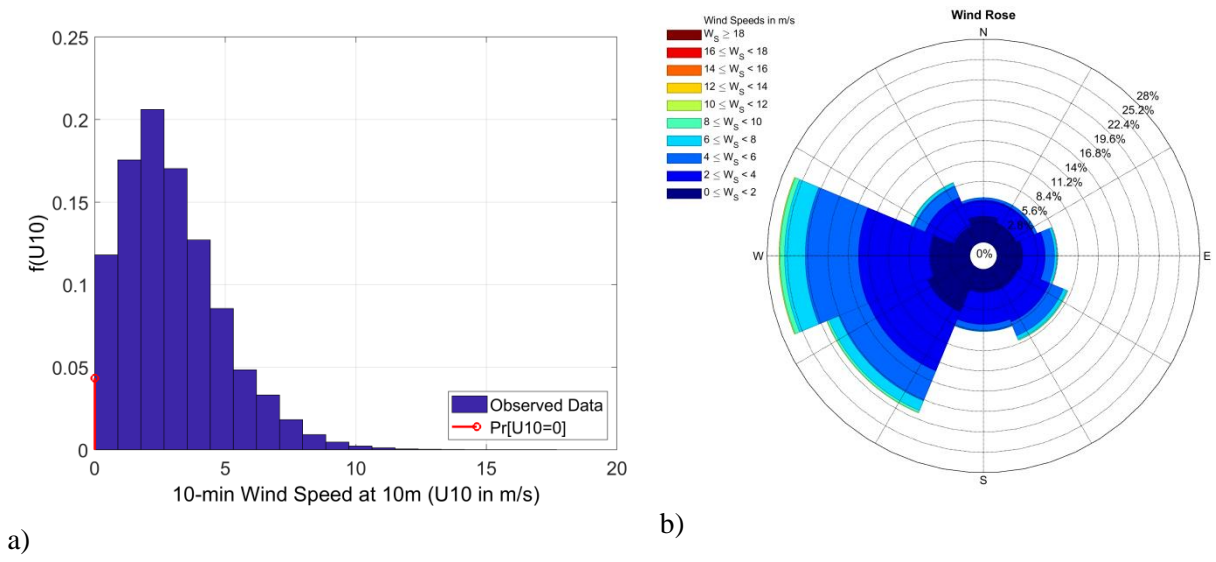
Figure 9. *Distributions of a) Wind Speed and b) Wind Direction (Wind Rose) for Marienberg*
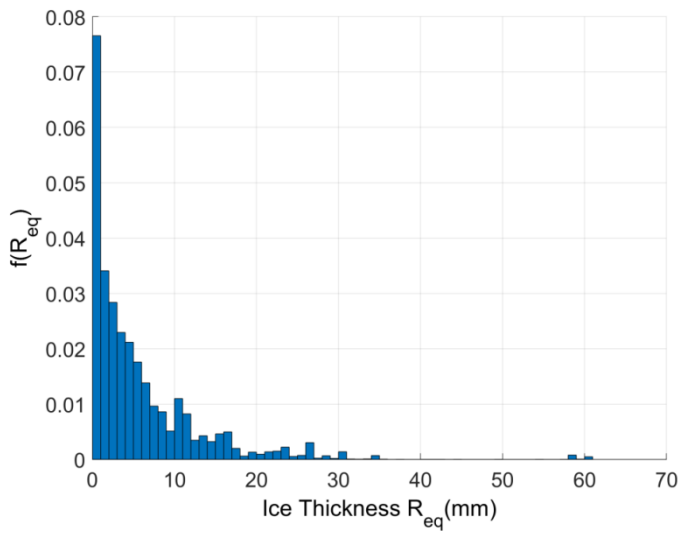
Figure 10. *Distribution of Ice Thickness (R_{eq}) for Marienberg*

The joint wind and ice thickness distribution is estimated by combining the distributions of wind speed (*Figure 9*a) and ice thickness (*Figure 10*). The result is given in Figure 11. During the estimation of the joint PDF, it was assumed that wind speed follows a Gumbel distribution while the ice thickness follows a lognormal distribution. Finally, it is noteworthy that the distribution corresponds to cases when there is ice (i.e. the values of z-axis are multiplied by 0.1889).
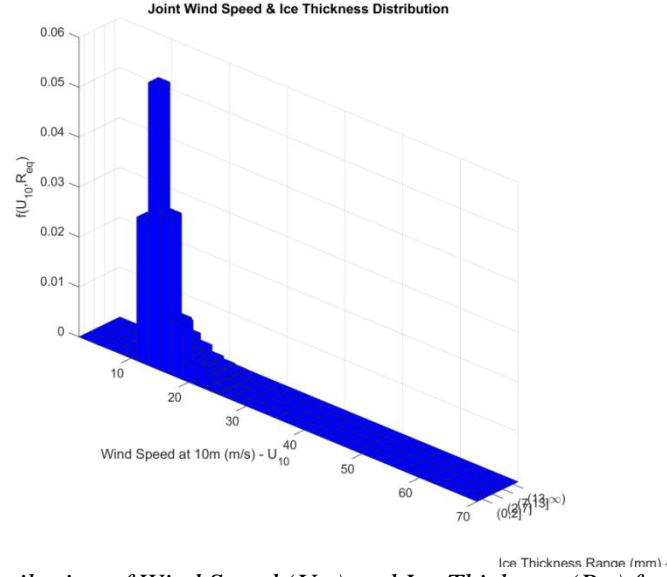
Figure 11. *Joint Distribution of Wind Speed (U$_{10}$) and Ice Thickness (R$_{eq}$) for Marienberg*

RISK ESTIMATION

The ultimate goal in a performance-based design is the estimation of the risk (of failure) of a specific structure given its structural strength and the hazard of its location. The probability of failure conditioned on the IM is specified by the fragility analysis as described in a previous Section. The frequency of IM occurrence, herein the climatic hazard, is estimated after the aforementioned statistical analyses of the meteorological data.

The combination of the information regarding fragility and hazard provides the risk of the structure. In other words, the risk, which is the probability of failure during the structure's service life, is estimated by integrating the structure's fragility function with the joint probability density function of wind and icing conditions for a given wind angle (θ):

$$\lambda = \int_{U=0}^{+\infty} \int_{R_{eq}=0}^{+\infty} P\big(D > C | U, R_{eq}\big) f\big(U, R_{eq}\big) \, \mathrm{d}U \, \mathrm{d}R_{eq} \qquad (18)$$

where: $P\big(D > C | U, R_{eq}\big)$ is the probability of failure (i.e. when demand D exceeds capacity C) for a given combination of wind speed U and ice thickness R_{eq} and it is actually provided by the fragility curve of the structure, and $f\big(U, R_{eq}\big)$ is the probability of occurrence of the combination of wind speed U and ice thickness R_{eq}, which corresponds to the hazard of the structure's location.

In order to account for the effect of wind direction Eq. (18) could be estimated for each of the wind directions (e.g. with wind angle θ) considered using the corresponding fragility curve. Then each value of $\lambda(\theta)$ is multiplied by the probability of occurrence of the corresponding wind direction $p(\theta)$ and finally the total probability λ is given by the equation:

$$\lambda = \sum_{\theta=1}^{n} p_\theta \lambda_\theta \qquad (19)$$

It should be mentioned here that the orientation of the tower (as part of a transmission line) was assumed to be N-S (*Figure 12*). Furthermore, as already stated, due to tower's symmetry, the three scenarios of wind angle of attack considered herein are sufficient to capture all the possible wind angles (directions) as shown in the wind roses. In terms of notation, a wind angle of 0° (i.e. wind of North direction) was considered to be longitudinal to the line while a wind angle of 90° (i.e. wind of East direction) was considered to be transversal to the line.
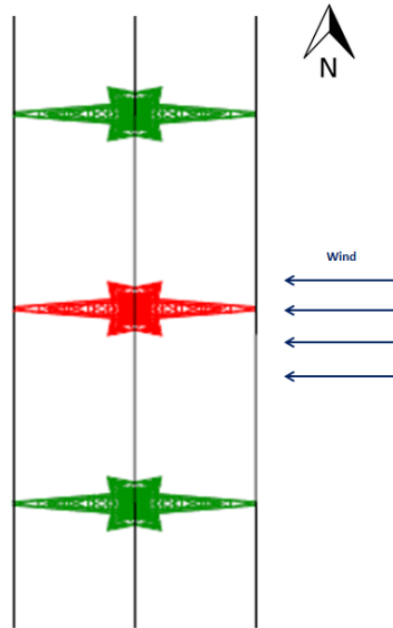
Figure 12. *Power line (and Transmission Towers) orientation*

The probability λ is usually an annualized probability of failure, thus the reciprocal of its value corresponds to the Return Period (RP) of failure in years:

$$RP = \frac{1}{\lambda}$$ (20)

Finally, the probability of failure during the service life of structure T can be estimated by the equation:

$$P_{fail} = 1 - e^{-\lambda T}$$ (21)

The results of risk estimation for both versions of the tower are shown in Table 2.

Table 2. *Risk Estimation Results*

	Initial Tower	Corroded Tower
λ (yr^{-1})	1.84E-04	7.37E-04
Return Period (yrs)	5435.97	1357.08
Probability of Failure in 60yrs	0.0110	0.0432

It is obvious that the risk values are consistent with the strength of the towers. In specific, the corroded tower has approximately 4 times higher probability of failure than the initial one, pointing out the effect of aging on steel towers.

CONCLUSIONS
Accurate estimation of risk even for a single transmission tower is a difficult process that requires three distinct steps, namely careful structural modelling, weather data processing and ice accretion modelling. Lattice tower models are sensitive to the modelling of member buckling and the incorporation of conductor loads under wind and ice conditions. Meteorological data from weather stations can provide the basis for establishing the climatic hazard of the site, yet ice accretion is practically never measured, and thus requires modelling to be extracted. Based on such data, the probability of occurrence of adverse weather conditions, namely high wind speed and ice accretion on the power line can be calculated and the probability of failure (i.e. risk) can be estimated by integrating the fragility results with the climatic hazard.

For the case at hand, the results confirm the significant effect of wind on steel lattice structures, especially when it is combined with ice accretion. Specifically, the probability of failure tends to increase as ice accumulates on the structure for any given wind speed value. Overall, the results show small probability of failure for the Danube type tower corresponding to a return period greater than the usual design life of such structures, yet not necessarily of sufficient safety for critical infrastructure. Nevertheless, the above probability (even still small) is increased for the case of a corroded tower with the same typology. This finding should be attributed to the lower strength of the corroded tower pointing out the effects of ageing on steel lattice structures.

The methodology presented herein could be applied to other sites for the same tower model or other types of towers in order to estimate the risk of entire power transmission lines. This risk estimation could be used as a useful decision tool by power companies for decision making regarding the maintenance or upgrade of their network.

REFERENCES
ANGELHY Deliverable 1.3 (2019) Report on analysis and design of 6 case studies. Research Program of the Research Fund for Coal and Steel ANGELHY, Grant Agreement Number: 753993, European Commission, Brussels, Belgium.

Bakalis, K., & Vamvatsikos, D. (2018). Seismic fragility functions via nonlinear response history analysis. Journal of structural engineering, 144(10).

Baker, J. W. (2015). Efficient analytical fragility function fitting using dynamic structural analysis. Earthquake Spectra, 31(1), 579-599.

Bezas, M. Z., Tibolt, M., Jaspart, J. P., & Demonceau, J. F. (2019). Critical assessment of the design of an electric transmission tower. In 9th International Conference on Steel and Aluminium Structures, Bradford 3-5 July 2019.

Braconi et al. (2013) Optimising the seismic performance of steel and steel-concrete structures by standardising material quality control (OPUS), Research Program of the Research Fund for Coal and Steel, Grant Agreement Number: RFSR-CT-2007-00039, European Commission, Brussels, Belgium.

CEN: EN 50341-1. (2012) Overhead electrical lines exceeding AC 1 kV - Part 1: General requirements - Common specifications. Comité Européen de Normalisation (CEN), Brussels, Belgium.

Cornell, C. A., Jalayer, F., Hamburger, R. O., & Foutch, D. A. (2002). Probabilistic basis for 2000 SAC federal emergency management agency steel moment frame guidelines. Journal of structural engineering, 128(4), 526-533.

Cuchapin, J. (2018) Fundamental concepts of sag-tension relationship in transmission and distribution lines. Available online at: https://electricalengineerresources.com/2018/01/02/complete-sag-tension-relationship-in-transmission-and-distribution-lines-concepts/ (Accessed September 2019)

EN 1991-1-4 (2005) Eurocode 1: Actions on structures - Part 1-4: General actions - Wind actions. Comité Européen de Normalisation (CEN), Brussels, Belgium.

EN 1993-3-1 (2006) Design of steel structures - Part 3-1: Towers, masts and chimneys – Towers and masts. Comité Européen de Normalisation (CEN) Brussels, Belgium.

EN 50341-1 (2012) Overhead electrical lines exceeding AC 1 kV - Part 1: General requirements - Common specifications.

EN 50341-2-4 (2016) Overhead electrical lines exceeding AC 1 kV - Part 2-4: National Normative Aspects (NNA) for Germany (based on EN 50341-1:2012).

EN 12500:2000 Protection of metallic materials against corrosion – Corrosion likelihood in atmospheric environment – Classification, determination and estimation of corrosivity of atmospheric environments.

EN ISO 9223. Corrosion of Metals and Alloys: Corrosivity of Atmospheres: Classification; European Committee for Standardization (CEN): Brussels, Belgium, 1992.

EN ISO 9224. Corrosion of Metals and Alloys: Corrosivity of Atmospheres: Guiding Values for the Corrosivity Categories; European Committee for Standardization (CEN): Brussels, Belgium, 1992.

EN ISO 9225. Corrosion of Metals and Alloys: Corrosivity of Atmospheres: Measurement of Pollution; European Committee for Standardization (CEN): Brussels, Belgium, 1992.

EN ISO 9226. Corrosion of Metals and Alloys: Corrosivity of Atmospheres: Determination of Corrosion Rate of Standard Specimens for the Evaluation of Corrosivity; European Committee for Standardization (CEN): Brussels, Belgium, 1992.

Fu, X., Li, H. N., & Li, G. (2016). Fragility analysis and estimation of collapse status for transmission tower subjected to wind and rain loads. Structural safety, 58, 1-10.

Fu, X., Li, H. N., Tian, L., Wang, J., & Cheng, H. (2019). Fragility analysis of transmission line subjected to wind loading. Journal of Performance of Constructed Facilities, 33(4).

IEC 61400-1. (2005) Wind Turbines-Part 1: Design Requirements. International Electrotechnical Commission, Geneva, Switzerland.

Jalayer, F., & Cornell, C. A. (2009). Alternative non-linear demand estimation methods for probability-based seismic assessments. Earthquake Engineering & Structural Dynamics, 38(8), 951-972.

Jones, K. F. (1998). A simple model for freezing rain ice loads. Atmospheric research, 46(1-2), 87-97.

Jonkman, B. J., & Kilcher, L. (2012). TurbSim user's guide: version 1.06. 00. National Renewable Energy Laboratory: Golden, CO, USA.

Kiessling, F., Nefzger, P., Nolasco, J. F., & Kaintzyk, U. (2003). Overall planning. In Overhead Power Lines (pp. 1-23). Springer, Berlin, Heidelberg.

Klinger, C., Mehdianpour, M., Klingbeil, D., Bettge, D., Häcker, R., & Baer, W. (2011). Failure analysis on collapsed towers of overhead electrical lines in the region Münsterland (Germany) 2005. Engineering Failure Analysis, 18(7), 1873-1883.

Mazzoni, S.; McKenna, F.; Scott, M.; Fenves, G. (2006) Open system for earthquake engineering simulation. User Command-Language Manual, Report NEES grid-TR 2004-21, Berkeley, CA: Pacific Earthquake Engineering Research, University of California, Retrieved http://opensees.berkeley.edu

Mohammadi Darestani, Y., Shafieezadeh, A., & Cha, K. (2020). Effect of modelling complexities on extreme wind hazard performance of steel lattice transmission towers. Structure and Infrastructure Engineering, 16(6), 898-915.

Paschen, R., Pezard, J., & Zago, P. (1988). Probabilistic Evaluation on Test Results of Transmission Line Towers. In CIGRE International Conference on Large High Voltage Electric Systems.

Rezaei, S. N. (2017). Fragility assessment and reliability analysis of transmission lines subjected to climatic hazards. McGill University (Canada).

Tibolt M., Bezas M.-Z., Vayas I., Jaspart J.-P., (2021), The design of a steel lattice transmission tower in Central Europe, Ernst & Sohn, ce/papers, Special Issue: EUROSTEEL 2021 Sheffield — Steel's coming home, Vol. 4, Issue 2 – 4, pp. 243-248.

Veletsos, A.S.; Darbre, G.R. (1983) Dynamic stiffness of parabolic cables Earthquake Engineering and Structural Dynamics 11, 367-401.

Zhang, W., Zhu, J., Liu, H., & Niu, H. (2015). Probabilistic capacity assessment of lattice transmission towers under strong wind. Frontiers in Built Environment, 1, 1-12.